

Assessing Optimal Implant-Prosthetic Rehabilitation in the Atrophic Mandible through Virtual Bone Augmentation: A Finite Element Study

Sînziana Anca Butnaru-Moldoveanu ^{1,*}, Florin Munteanu ^{1,*} and Norina Consuela Forna ²

¹ Department of Biomedical Sciences, Faculty of Medical Bioengineering, University of Medicine and Pharmacy “Grigore T. Popa”, 9-16 M. Kogalniceanu St., 700454 Iasi, Romania

² Department of Implantology, Removable Dentures, Dentures Technology, Faculty of Dental Medicine, University of Medicine and Pharmacy “Grigore T. Popa”, 16 University St., 700115 Iasi, Romania;

Abstract: The scope of our study was to analyze the impact of implant prosthetic rehabilitation, in bilateral terminal partial edentulism with mandibular bone atrophy, and potential benefits of mandibular bone augmentation through finite element analysis. A 3D mandible model was made using patient-derived cone-beam computed tomography (CBCT) images, presenting a bilateral terminal edentation and mandibular atrophy. A virtual simulation of bone augmentation was then made. Implant-supported restorations were modeled for each edentulous area. Forces corresponding to the pterygoid and the masseter muscles, as well as mastication conditions for each quadrant, were applied. The resorbed mandible presented high values of strain and stress. A considerable variation between strain values among the two implant sites in each quadrant was found. In the augmented model, values of strain and stress showed a uniformization in both quadrants. Virtually increasing bone mass in the resorbed areas of the mandible showed that enabling larger implants drastically reduces strain and stress values in the implant sites. Also, although ridge height difference between the two quadrants was kept even after bone augmentation, there is a uniformization of the strain values between the two implant sites in each of the augmented mandible quadrants.

Keywords: finite element analysis; implant-supported restorations; bone resorption; bone augmentation; strain

1. Introduction

Implant-prosthetic rehabilitation has become a successful and highly predictable method used for restoring the functions of the stomatognathic system and improving the quality of the patient's life [1–3].

However, in the partially edentulous mandible with bone atrophy, a favorable bone volume and density is a prerequisite for achieving a successful implant-prosthetic rehabilitation [3,4]. In such cases, the placement of standard length implants is often prohibited by an insufficient height of the alveolar ridge [4]. Modern alveolar bone addition techniques can lead to the successful restoration of bone volume, creating the optimal geometry for the use of a larger dental implant [4]. Yet, in the posterior mandible, bone augmentation has been associated with a higher rate of peri-implant marginal bone loss, donor site morbidity, pain, increased costs, and duration of treatment [4–6].

In this case, short implants can be a viable solution in implant-prosthetic rehabilitation of the edentulous mandible with bone atrophy [7–9]. The development of surface treatment technologies,

high-performance materials, and design of microtopography of implants have helped to increase the reliability of short implants [7–10].

Oral rehabilitation becomes more challenging in the context of bilateral terminal edentulism. Further, as there are still insufficient data that could determine the optimal treatment, whether it would be rehabilitation using short implants or bone augmentation that would allow the use of longer implants, clinicians often face problematic situations [3]. However, some studies suggest that short implants may be more advantageous than longer implants placement following bone augmentation because of the reduced number of complications [7,8,11,12]. In comparison with sandwich osteotomy and delayed implant placement, prosthetic rehabilitation of the partially edentulous atrophic mandible with short implants has been shown to have a comparable survival rate [11]. Moreover, short implants placed in an atrophic ridge and long implants placed after alveolar bone augmentation have been reported to present similar short-term peri-implant alveolar bone loss, regardless of the arch [7].

While these clinical studies offer valuable information, in complex rehabilitation cases, there is yet to be a consensus or a guideline that would offer long term success of prosthetic implant rehabilitation. Therefore, the question is whether or not bone augmentation is necessary to enable larger implants to be used when smaller implants may perform comparably and avoid complications from preliminary surgical procedures in complex cases, such as bilateral terminal edentulism with mandibular bone atrophy.

To the best of our knowledge, no previous finite element studies have yet to explore implant-prosthetic rehabilitation in the posterior mandible with bilateral terminal edentation and bone atrophy.

The scope of our study was to analyze the impact of implant prosthetic rehabilitation in bilateral terminal partial edentulism with mandibular bone atrophy and potential benefits of mandibular bone augmentation through finite element analysis (FEA).

2. Materials and Methods

A mandible 3D model was made using patient-derived cone-beam computed tomography (CBCT) images. The clinical model used presented a bilateral edentation of class I Kennedy. The mandible was also characterized by mandibular atrophy, bone field class II (bone height > 10 mm, bone crest width 2.5–5 mm), by the Misch & Judy classification (1987) [13]. Ridge height in the third quadrant at implant sites was 2.4 mm higher than the alveolar ridge in the fourth quadrant. The 3D reconstruction of the mandible and the remaining teeth was performed using Slicer3D (<http://www.slicer.org>) with further editing in Autodesk Fusion 360 (Autodesk, Inc., San Rafael, CA, USA) and Autodesk Inventor Professional version 2017 (Autodesk, Inc., San Rafael, CA, USA), as can be seen in Figure 1. The obtained model was then modified, simulating a bone augmentation in the posterior mandible. The height of the mandible ridge at the implant sites was increased by 3 mm, as shown in Figure 2. Both mandible models consisted of two macro-structures, a cortical bone layer with a 2 mm thickness, and an internal cancellous bone, as well as gingival tissue with a thickness of 2 mm and periodontal ligaments with a thickness of 0.2 mm (Figure 2).

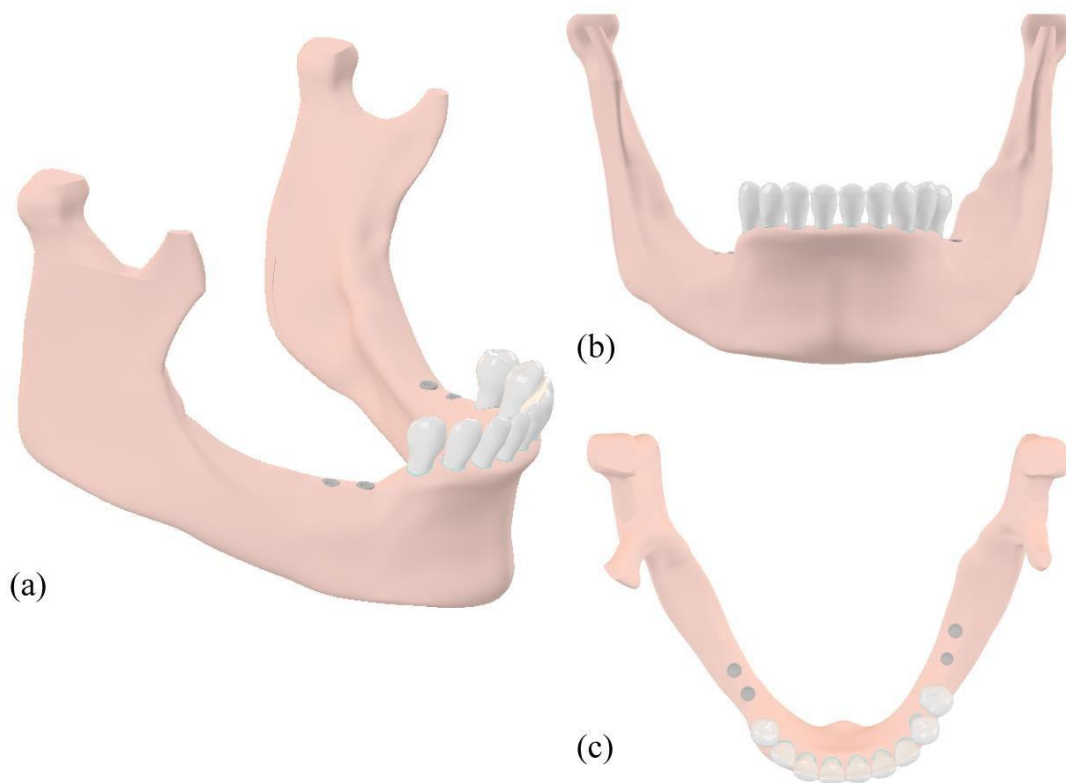


Figure 1. Detailed views of the 3D model of the resorbed and the virtually augmented mandible with implants placed in sites 3.6, 3.7, 4.5, and 4.6, and remaining dentition. (a) Perspective view of modeled mandible with bone resorption and bilateral posterior edentation with implants placed. (b) Front view of modeled mandible with bone resorption and bilateral posterior edentation with implants placed. (c) Top view of modeled mandible with bone resorption and bilateral posterior edentation with implants placed.

Implant-supported restorations were modeled for each edentulous area, consisting of implant, abutment, abutment screw, cement layer, and splinted ceramic crowns. In the atrophied mandible, implants measured 3.75 mm in diameter (D) and 8 mm in length (L) for implant sites 3.7, 4.5, 4.6, and 3.3 mm D with 10 mm L for implant site 3.6. These measurements were planned according to the available alveolar bone dimensions. In the virtually augmented mandible, all implants measured 4.2 mm D and 11.5 mm L.

Simulations of physiological loading of the 3D models were performed using Simulation Mechanical version 2017 (Autodesk, Inc., San Rafael, CA, USA). For all simulation scenarios, a static model with linear and elastic material properties was selected. The mechanical properties of the assigned materials are presented for each element of the 3D analysis assembly in Table 1.

The mandibular model was fixed in the simulation environment at the temporal–mandibular joint surfaces, with rotation restrictions around the Y and Z axes, to simulate the anatomical articulation of the structure and allow for physiological type rotation in the sagittal plane during mastication (Figure 3). Because the study model presented bilateral terminal edentation, restrictions were set on each one of the ceramic upper restorations at a time, simulating mastication conditions for each quadrant. Masticatory type forces corresponding to the pterygoid muscles (P) of 145 N and the masseter muscles (M) of 151 N were applied (Figure 3) [14].

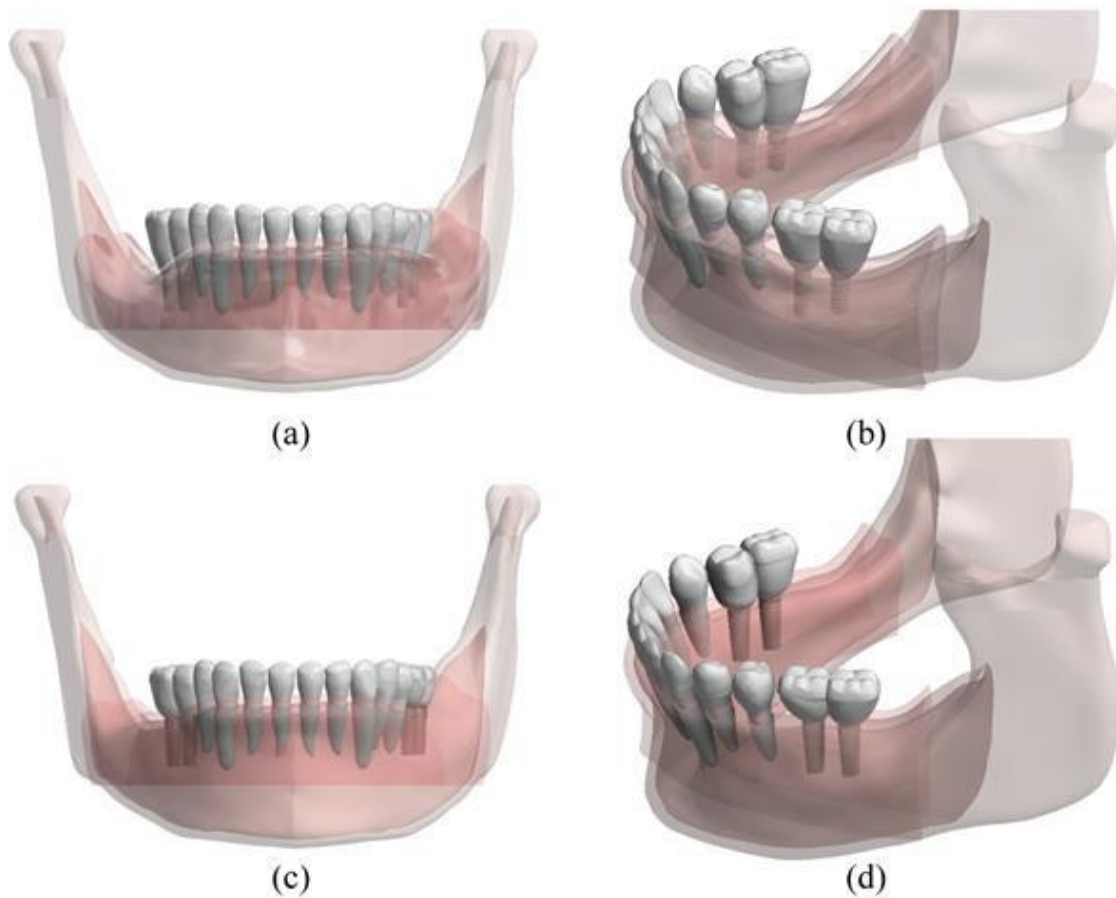


Figure 2. Detailed views of the 3D model of the resorbed and the virtually augmented mandible with modeled implant-supported restorations, remaining dentition, periodontal ligaments, gingiva, cortical, and cancellous bone layers. (a) Front view of complete model of the resorbed mandible with placed implant-supported restorations (b) Perspective view of complete model of the resorbed mandible with placed implant-supported restorations. (c) Front view of complete modeled mandible with simulated bone augmentation and placed implant-supported restorations. (d) Perspective view of complete modeled mandible with simulated bone augmentation and placed implant-supported restorations.

Table 1. Material properties.

Material	Young's Modulus (MPa)	Poisson Coefficient
Cortical bone [15–17]	13,700	0.3
Cancellous bone [17,18]	1370	0.3
Gingiva [19]	19.6	0.3
Dentina [20]	18,600	0.31
Periodontal ligament [21]	69	0.45
Ceramic [22]	140,000	0.28
Ti-6Al-4V [23]	110,000	0.35
Cement [24]	10,760	0.35

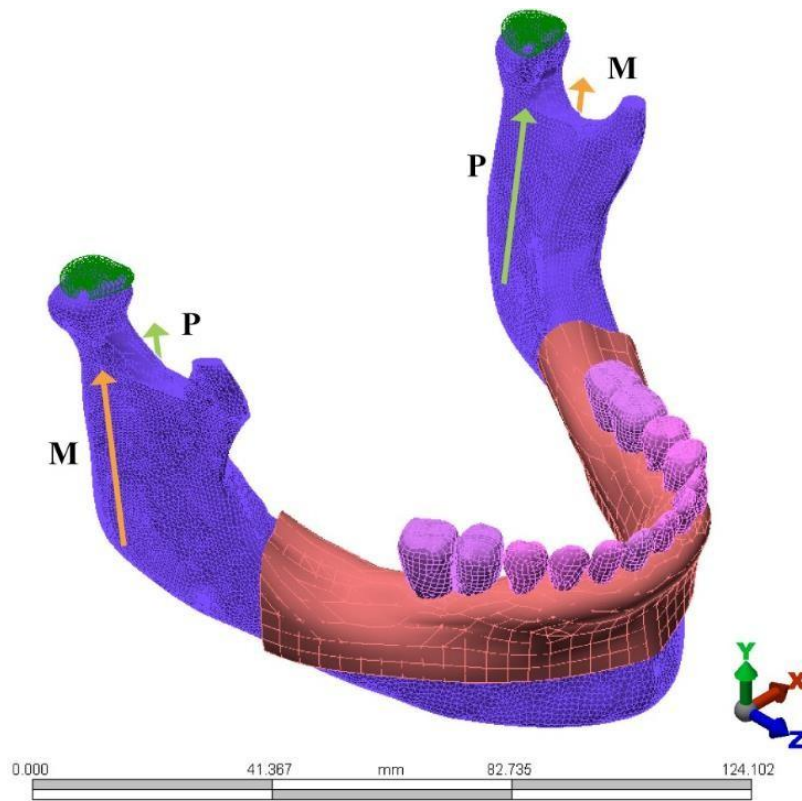


Figure 3. Complete mandible assembly in the simulation environment with applied forces corresponding to pterygoid muscles (P) and the masseter muscles (M) and restrictions at the temporomandibular joint surfaces.

The failure criteria for materials are generally expressed in terms of stress or strain. The biological response of bone tissue to loads applied depends, according to Frost's "mechanostat" theory, on the strain recorded in the tissue [25,26]. The octahedral shear (equivalent) strain is considered to be the most relevant strain for this theory and to be far more conservative than other types of strain such as maximum compression strain. According to the mechanostat theory, the recommended range of strain is 1000–3000 $\mu\epsilon$. Below 1000 $\mu\epsilon$, bone tissue experiences stress shielding, leading to bone atrophy. Above 3000 $\mu\epsilon$, the bone tissue is exposed to pathologic overload, which leads to bone damage and absorption [27]. In the simulations of this study, the octahedral shear (equivalent) strain was tracked.

For calculation of the octahedral shear strain, strain component tensors, ϵ_{xx} , ϵ_{yy} , ϵ_{zz} , γ_{xy} , γ_{yz} , and γ_{zx} , were recorded near the implant site. These strain component tensors were then used to calculate the principal strains (ϵ_1 , ϵ_2 , ϵ_3), through matrix diagonalization, using a modified version of Cauchy's symmetric strain tensor [28] as follows:

$$T_{\epsilon} = \begin{bmatrix} \epsilon_{xx} & \frac{1}{2}\gamma_{xy} & \frac{1}{2}\gamma_{xz} \\ \frac{1}{2}\gamma_{yx} & \epsilon_{yy} & \frac{1}{2}\gamma_{yz} \\ \frac{1}{2}\gamma_{zx} & \frac{1}{2}\gamma_{zy} & \epsilon_{zz} \end{bmatrix} \quad (1)$$

The principal strains obtained, ϵ_1 , ϵ_2 , and ϵ_3 , were then used to obtain the octahedral shear (equivalent) strain as follows:

$$\epsilon_{oct} = \frac{2}{3} \sqrt{(\epsilon_1 - \epsilon_2)^2 + (\epsilon_2 - \epsilon_3)^2 + (\epsilon_3 - \epsilon_1)^2}. \quad (2)$$

Surface averaging of each octahedral shear strain value calculated for each point was done to avoid numerical artifacts of local peak values.

3. Results

In the resorbed mandible model, strain values in the bone tissue were found to be highest in both quadrants of the mandible in comparison with the virtually bone augmented model, as shown in Figure 4.

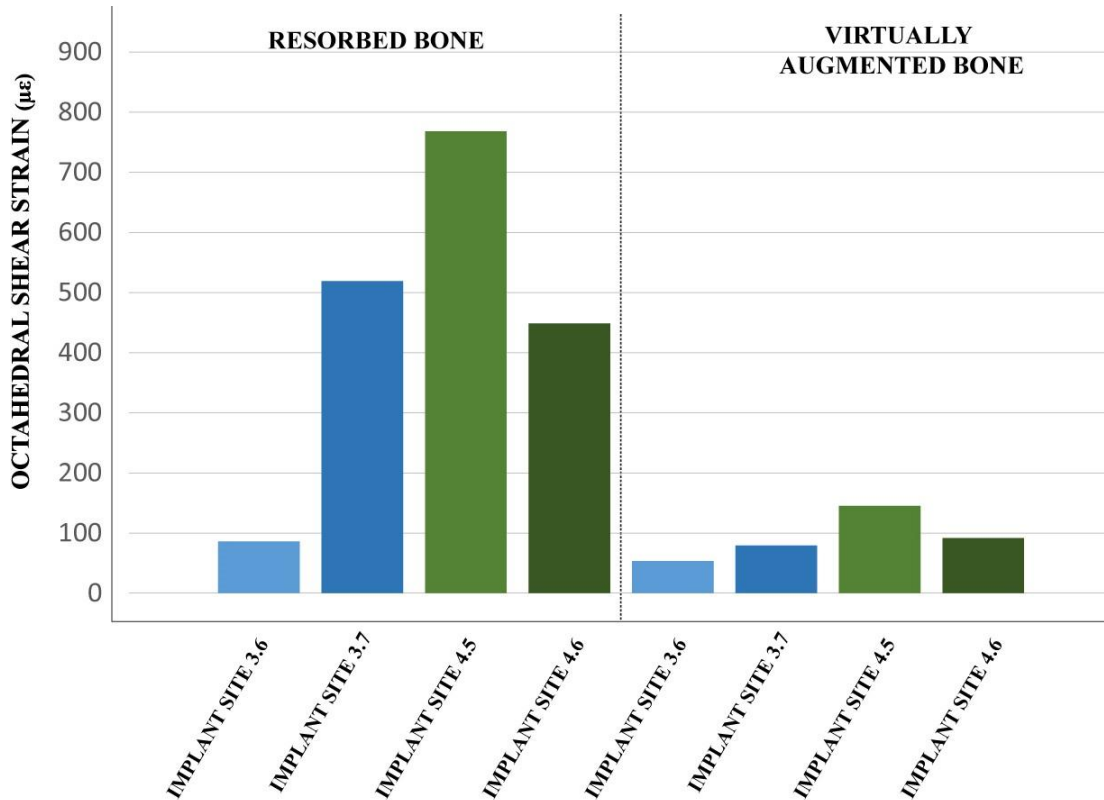


Figure 4. Octahedral shear strain in the resorbed and virtually bone augmented mandible for implant-supported restoration in the third and fourth quadrant.

There was also a considerable variation between strain values among the two implant sites in each mandible quadrant in the resorbed mandible. Moreover, where the 3.3D/10L implant was used in implant site 3.6, strain values obtained were the smallest, as opposed to the other implant sites where the 3.7D/8L implants were used.

After simulation of bone augmentation, strain values decreased in all implant sites. In each quadrant, differences in strain values between each implant site also decreased (Figure 4).

Stress was concentrated at crestal bone level in all simulated cases, as shown in Figure 5. The highest values of stress were recorded in the resorbed mandible model. Between the two quadrants of the resorbed model, there is still a considerable variation of stress values. In the virtually bone augmented mandible mode, as stress and strain values decreased, the area of distribution increased as more bone was engaged. The values of stress between the two quadrants of the augmented model were similar (Figure 5).

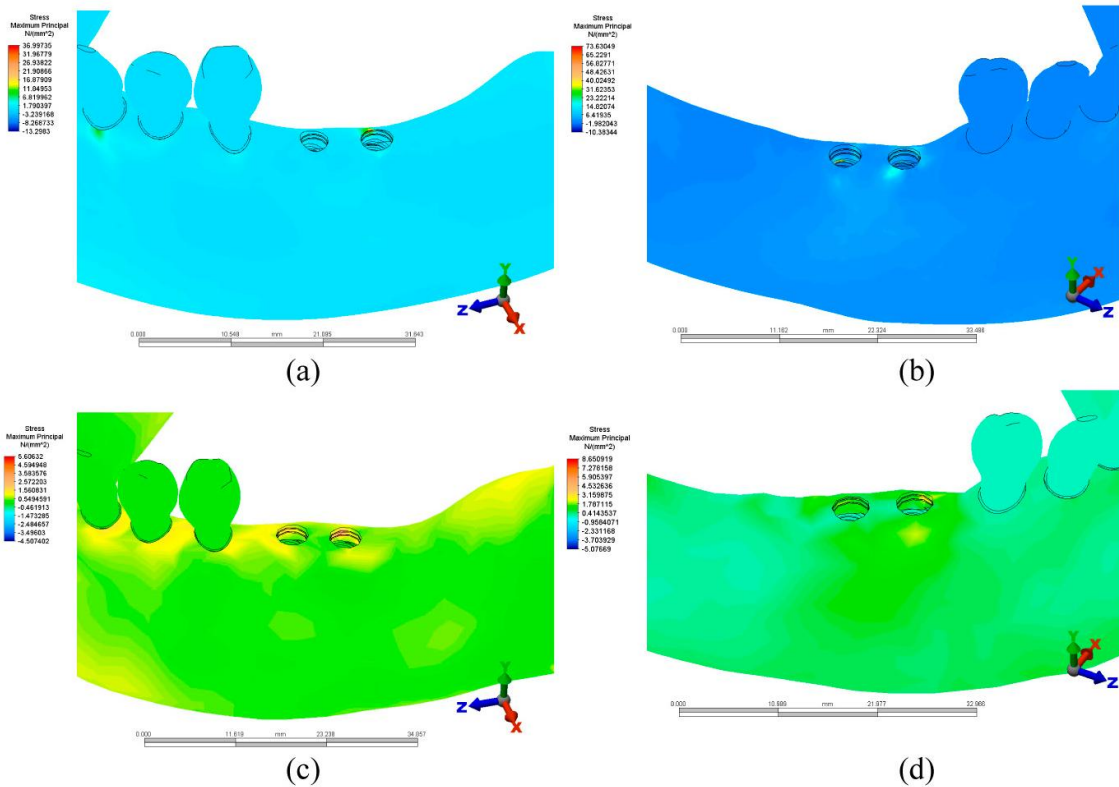


Figure 5. Maximum principal stress values and distribution in mandibular bone in the resorbed model for the third (a) and fourth (b) quadrant and the virtually bone augmented model for the third (c) and fourth (d) quadrant.

4. Discussion

The long-term survival of implant-supported restorations depends on bone quality and quantity as well as implant dimensions [29,30]. High-stress concentration areas in addition to high strain values owing to excessive implant loading are related to bone resorption [30–34]. Bone homeostasis is achieved, according to Frost’s “mechanostat theory”, when bone tissue responds favorably to the forces transferred through the implant and strain values fall between 1000 $\mu\epsilon$ and 1500 $\mu\epsilon$ [25,26]. Bone remodeling occurs when strain values are in the 1500 $\mu\epsilon$ –3000 $\mu\epsilon$ interval, but above these values, the risk of bone resorption or even fracture rises significantly [25,26].

The results of our study showed that, by virtually increasing bone mass and allowing for larger implants to be used, strain values decreased in both quadrants. Although strain values for both resorbed and bone augmented mandible were far under the lower limit of the bone homeostasis interval, the variability of muscle forces in current literature, as well as an additional effect of other masticatory muscles, must be taken into account [35].

Studies that have reported values above the lower limit of the homeostasis interval have used sections of the mandible bone and applied a set value of force directly on the abutment or, in some cases, on the ceramic upper restoration [36–39]. This is considered an oversimplification in the analysis and, although it may show a trend of the strain values in the bone tissue, it may also lead to artifacts or unreliable results [35–40]. Moreover, there is currently a high variability regarding the magnitude of forces applied directly on implant-supported restorations having a large influence of the strains exerted on the bone tissue [40].

In a study on the importance of input variables in mandible biomechanics analysis, where a complete mandible was modeled with a full dental arch, strain values reported were similar to those obtained in our study [35]. Our results also show that, after the simulated bone augmentation, there is a uniformization of the strain values between the two implant sites in each of the mandible quadrants.

Stress values in the bone augmented model exhibited the same pattern. This is because of the increase of implant diameter and length, as well as an increase in bone volume. Besides the dimensional factor of the implants, attention needs to be given to the virtually augmented bone dimensions. The increase of bone volume seems to minimize the position effect of the teeth on the strain values recorded in the bone tissue. The small differences that do exist in strain between each of the implant sites may be because of the position that leads to a specific physiological load [41–43]. This may suggest that, in the absence of bone augmentation, further consideration needs to be given to the placement of the implant in atrophic ridges.

In the resorbed mandible model, higher stress values were obtained compared with the simulated bone augmented mandible model. Increasing the implant diameter from 3.3 mm/3.75 mm to 4.2 mm and the length from 8 mm/10 mm to 11.5 mm led to a considerable decrease in stress, as well as a favorable distribution at the crestal level. This is in accordance with several studies that suggest that increasing the diameter and length of the implant leads to lower stress values in the mandibular bone [35,43,44].

In our study, the distribution of stress was found to be similar in the resorbed and bone augmented ridge, as stress was concentrated at the crestal level. This is because of the difference between the elastic modulus of the cortical and cancellous bone. Owing to the increased stiffness provided by a higher elastic modulus in the cortical bone tissue, stress concentrates at the crestal bone level. These findings are consistent with current studies, which suggest that this type of stress concentration is more influenced by the mechanical properties of the bone tissue as well as the type of loading applied [45,46]. Moreover, as high stress and strain values are found at crestal level, which may lead to bone resorption and implant failure, clinicians should carefully plan implant restorations in both augmented and resorbed ridges.

Simulating a bone augmentation in a real clinical case allowed for a comprehensive assessment of rehabilitation possibilities. This method may be further developed as a standardized method of evaluation, allowing for individual patient FEA simulations. However, the diversity of bone augmentation techniques may be challenging to assess in FEA studies. Moreover, from a clinical point of view, it is difficult to evaluate the performance of any bone augmentation technique while ensuring an increased implant success rate [4,6]. The clinical evidence of oral rehabilitation success in mandibular bilateral terminal edentulism with bone atrophy is scarce. However, our results are in accordance with the reported clinical studies, suggesting that bone augmentation may be beneficial to the long-term survival of dental implants [3,30].

Another important aspect of the studied mandible is the absence of an implant restoration of the second molar in the fourth quadrant. The need to replace the tooth with an implant-prosthetic restoration remains a topic of debate [47,48]. However, as the decision to not restore the missing second molar is a common practice, it was important to keep this detail to ensure input variables in the finite element study are as close to clinical reality as possible.

5. Conclusions

Virtually increasing bone mass in the resorbed areas of a CBCT derived mandible model with bilateral partial edentulism showed that enabling larger implants drastically reduces strain and stress values in the implant sites. Also, although the ridge height difference between the two quadrants was kept even after bone augmentation, there is a uniformization of the strain values between the two implant sites in each of the augmented mandible quadrants. Stress values in the bone augmented model exhibited the same pattern. In the resorbed mandible, values of strain varied greatly between each implant site in the two quadrants, even where implants of the same dimensions were used. These findings suggest that bone augmentation may be favorable to the long-term survival of implant-supported restorations. This research may be further developed to offer a comprehensive individualized method of evaluation. This may allow clinicians to assess each patient through individual finite element

analysis simulations. Further studies need to address complex rehabilitation cases that reflect real clinical aspects, using patient-specific data to ensure the accuracy and validity of results.

Author Contributions: All authors have equally contributed to the completion of this research and article. All authors have read and agreed to the published version of the manuscript.

Funding: This research received no external funding.

Conflicts of Interest: The authors declare no conflict of interest.

References

1. Buser, D.; Sennerby, L.; De Bruyn, H. Modern implant dentistry based on osseointegration: 50 years of progress, current trends and open questions. *Periodontol. 2000* **2017**, *73*, 7–21. [[CrossRef](#)]
2. Chappuis, V.; Buser, R.; Bragger, U.; Bornstein, M.M.; Salvi, G.E.; Buser, D. Long-term outcomes of dental implants with a titanium plasma-sprayed surface: A 20-year prospective case series study in partially edentulous patients. *Clin. Implant Dent. Relat. Res.* **2013**, *15*, 780–790. [[CrossRef](#)]
3. Merli, M.; Moscatelli, M.; Pagliaro, U.; Mariotti, G.; Merli, I.; Nieri, M. Implant prosthetic rehabilitation in partially edentulous patients with bone atrophy. An umbrella review based on systematic reviews of randomised controlled trials. *Eur. J. Oral Implantol.* **2018**, *11*, 261–280.
4. Herford, A.S.; Nguyen, K. Complex bone augmentation in alveolar ridge defects. *Oral Maxillofac. Surg. Clin. N. Am.* **2015**, *27*, 227–244. [[CrossRef](#)]
5. Camargo, I.B.; Van Sickels, J.E. Surgical complications after implant placement. *Dent. Clin. N. Am.* **2015**, *59*, 57–72. [[CrossRef](#)]
6. Elnayef, B.; Monje, A.; Gargallo-Albiol, J.; Galindo-Moreno, P.; Wang, H.L.; Hernández-Alfaro, F. Vertical Ridge Augmentation in the Atrophic Mandible: A Systematic Review and Meta Analysis. *Int. J. Oral Maxillofac. Implant.* **2017**, *32*, 291–312. [[CrossRef](#)]
7. Amine, M.; Guelzim, Y.; Benfaida, S.; Bennani, A.; Andoh, A. Short implants (5–8 mm) vs. long implants in augmented bone and their impact on peri-implant bone in maxilla and/or mandible: Systematic review. *J. Stomatol. Oral Maxillofac. Surg.* **2018**, *120*, 133–142. [[CrossRef](#)]
8. Mendonça, J.A.; Francischone, C.E.; Senna, P.M.; Matos de Oliveira, A.E.; Sotto-Maior, B.S. A retrospective evaluation of the survival rates of splinted and non-splinted short dental implants in posterior partially edentulous jaws. *J. Periodontol.* **2014**, *85*, 787–794. [[CrossRef](#)] [[PubMed](#)]
9. Rossi, F.; Botticelli, D.; Cesaretti, G.; De Santis, E.; Storelli, S.; Lang, N.P. Use of short implants (6 mm) in a single-tooth replacement: A 5-year follow-up prospective randomized controlled multicenter clinical study. *Clin. Oral Implant. Res.* **2016**, *27*, 458–464. [[CrossRef](#)] [[PubMed](#)]
10. Alexandru, A.; Cimpoesu, R.; Melian, A.; Salceanu, M. Study on the behavior of dental alloy COCrWnBMOV in artificial saliva. *Rev. Chim.* **2019**, *70*, 165–168.
11. Starch-Jensen, T.; Nielsen, H.B. Prosthetic Rehabilitation of the Partially Edentulous Atrophic Posterior Mandible with Short Implants (≤ 8 mm) Compared with the Sandwich Osteotomy and Delayed Placement of Standard Length Implants (> 8 mm): A Systematic Review. *J. Oral Maxillofac. Res.* **2018**, *9*, e2. [[CrossRef](#)] [[PubMed](#)]
12. Clelland, N.; Chaudhry, J.; Rashid, R.G.; McGlumphy, E. Split-mouth comparison of splinted and nonsplinted prostheses on short implants: 3-year results. *Int. J. Oral Maxillofac. Implant.* **2016**, *31*, 1135–1141. [[CrossRef](#)] [[PubMed](#)]
13. Misch, C.E.; Judy, K.W. Classification of partially edentulous arches for implant dentistry. *Int. J. Oral Implantol.* **1987**, *4*, 7–13. [[PubMed](#)]
14. Correia, A.; Piloto, P.; Reis Campos, J.C.; Vaz, M. Finite element analysis of the mechanical behavior of a partially edentulous mandible as a function of cancellous bone density. *J. Dent. Sci.* **2009**, *24*, 22–27.
15. Bozkaya, D.; Muftu, S.; Muftu, A. Evaluation of load transfer characteristics of five different implants in compact bone at different load levels by finite elements analysis. *J. Prosthet. Dent.* **2004**, *92*, 523–530. [[CrossRef](#)] [[PubMed](#)]
16. Sevimay, M.; Turhan, F.; Kiliçarslan, M.A.; Eskitascioglu, G. Three-dimensional finite element analysis of the effect of different bone quality on stress distribution in an implant-supported crown. *J. Prosthet. Dent.* **2005**, *93*, 227–234. [[CrossRef](#)]

17. Chun, H.J.; Park, D.N.; Han, C.H.; Heo, S.J.; Heo, M.S.; Koak, J.Y. Stress distribution in maxillary bone surrounding overdenture implants with different overdenture attachments. *J. Oral Rehabil.* **2005**, *32*, 193–205. [[CrossRef](#)]
18. Papavasiliou, G.; Tripodakis, A.P.; Kamposiora, P.; Strub, J.R.; Bayne, S.C. Finite element analysis of ceramic abutment-restoration combinations for osseointegrated implants. *Int. J. Prosthodont.* **1996**, *9*, 254–260.
19. Reinhardt, R.A.; Krejci, R.F.; Pao, Y.C.; Stannard, J.G. Dentin stresses in post-reconstructed teeth with diminishing bone support. *J. Dent. Res.* **1983**, *62*, 1002–1008. [[CrossRef](#)]
20. Holmes, D.C.; Diaz-Arnold, A.M.; Leary, J.M. Influence of post dimension on stress distribution in dentin. *J. Prosthet. Dent.* **1996**, *75*, 140–147. [[CrossRef](#)]
21. Sato, Y.; Tsuga, K.; Abe, Y.; Asahara, S.; Akagawa, Y. Finite element analysis on preferable I-bar clasp shape. *J. Oral Rehabil.* **2001**, *28*, 413–417. [[CrossRef](#)] [[PubMed](#)]
22. Vaillancourt, H.; Pilliar, R.M.; Mccammond, D. Finite-element analysis of crestal bone loss around porous-coated dental implants. *J. Appl. Biomater.* **1995**, *6*, 267–282. [[CrossRef](#)] [[PubMed](#)]
23. Grandin, H.M.; Berner, S.; Dard, M. A review of titanium zirconium (TiZr) alloys for use in endosseous dental implants. *Materials* **2012**, *5*, 1348–1360. [[CrossRef](#)]
24. Souder, W.H.; Paffenbarger, G.C. Physical Properties of Dental Materials. In *National Bureau of Standards Circular No. C433*; Government Printing Office: Washington, DC, USA, 1992.
25. Frost, H.M. Bone mass and the mechanostat: A proposal. *Anat. Rec.* **1987**, *219*, 1–9. [[CrossRef](#)]
26. Frost, H.M. A 2003 update of bone physiology and Wolff's law for clinicians. *Angle Orthod.* **2004**, *74*, 3–15.
27. Piccinini, M.; Cugnoni, J.; Botsis, J.; Ammann, P.; Wiskott, A. Numerical prediction of peri-implant bone adaptation: Comparison of mechanical stimuli and sensitivity to modeling parameters. *Med. Eng. Phys.* **2016**, *38*, 1348–1359. [[CrossRef](#)]
28. McGarry, M.D.J.; Van Houten, E.E.W.; Perrañez, P.R.; Pattison, A.J.; Weaver, J.B.; Paulsen, K.D. An Octahedral Shear Strain Based measure of SNR for 3D MR Elastography. *Phys. Med. Biol.* **2011**, *56*, N153–N164. [[CrossRef](#)]
29. Miyamoto, I.; Tsuboi, Y.; Wada, E.; Suwa, H.; Iizuka, T. Influence of cortical bone thickness and implant length on implant stability at the time of surgery—clinical, prospective, biomechanical, and imaging study. *Bone* **2005**, *37*, 776–780. [[CrossRef](#)]
30. Berglundh, T.; Persson, L.; Klinge, B. A systematic review of the incidence of biological and technical complications in implant dentistry reported in prospective longitudinal studies of at least 5 years. *J. Clin. Periodontol.* **2002**, *29*, 197–212. [[CrossRef](#)]
31. Baqain, Z.H.; Moqbel, W.Y.; Sawair, F.A. Early dental implant failure: Risk factors. *Br. J. Oral Maxillofac. Surg.* **2012**, *50*, 239–243. [[CrossRef](#)]
32. Tonetti, M.S.; Schmid, J. Pathogenesis of implant failures. *Periodontol. 2000* **1994**, *4*, 127–138. [[CrossRef](#)] [[PubMed](#)]
33. Lee, J.H.; Frias, V.; Lee, K.W.; Wright, R.F. Effect of implant size and shape on implant success rates: A literature review. *J. Prosthet. Dent.* **2005**, *94*, 377–381. [[CrossRef](#)] [[PubMed](#)]
34. Almas, K.; Smith, S.; Kutkut, A. What is the Best Micro and Macro Dental Implant Topography? *Dent. Clin. N. Am.* **2019**, *63*, 447–460. [[CrossRef](#)] [[PubMed](#)]
35. Groning, F.; Fagan, M.; O'higgins, P. Modeling the Human Mandible Under Masticatory Loads: Which Input Variables are Important? *Anat. Rec.* **2012**, *295*, 853–863. [[CrossRef](#)] [[PubMed](#)]
36. Ueda, N.; Takayama, Y.; Yokoyama, A. Minimization of dental implant diameter and length according to bone quality determined by finite element analysis and optimized calculation. *J. Prosthodont. Res.* **2017**, *61*, 324–332. [[CrossRef](#)] [[PubMed](#)]
37. Korabi, R.; Shemtov-Yona, K.; Dorogoy, A.; Rittel, D. The failure envelope concept applied to the bone-dental implant system. *Sci. Rep.* **2017**, *7*, 2051. [[CrossRef](#)]
38. Nemat, S.; Khorrammehr, S. Three Dimensional Evaluation of a Dental Implant in Different Angles by Finite Element Method. *Bioeng. Res.* **2019**, *1*, 42–53.
39. Van Staden, R.C.; Guan, H.; Loo, Y.C. Application of the finite element method in dental implant research. *Comput. Methods Biomech. Biomed. Eng.* **2006**, *9*, 257–270. [[CrossRef](#)]
40. Rittel, D.; Shemtov-Yona, K.; Korabi, R. Engineering Dental Implants. *Curr. Oral Health Rep.* **2017**, *4*, 239–247. [[CrossRef](#)]

41. Misch, C.E. Single-tooth replacement: Treatment options. In *Misch CE. Contemporary Implant Dentistry*, 3rd ed.; Mosby: St. Louis, MO, USA, 2008; pp. 327–366.
42. Iegami, C.M.; Barbosa, W.F.; Furuyama, R.J.; Lima, J.R.; de Campos, T.T.; Minagi, S.; Tamaki, R. Masticatory efficiency in complete denture wearers with reduced dental arches—a randomised cross-over study. *J. Oral Rehabil.* **2014**, *41*, 619–623. [[CrossRef](#)]
43. Broadbent, J.M. Chewing and occlusal function. *Funct. Orthod.* **2000**, *17*, 34–39. [[PubMed](#)]
44. Li, T.; Hub, K.; Cheng, L.; Dinga, Y.; Ding, Y.; Shao, J.; Kong, L. Optimum selection of the dental implant diameter and length in the posterior mandible with poor bone quality—A 3D finite element analysis. *Appl. Math. Model.* **2011**, *35*, 446–456. [[CrossRef](#)]
45. Kang, N.; Wu, Y.Y.; Gong, P.; Yue, L.; Ou, G.M. A study of force distribution of loading stresses on implant-bone interface on short implant length using 3-dimensional finite element analysis. *Oral Surg. Oral Med. Oral Pathol. Oral Radiol.* **2014**, *118*, 519–523. [[CrossRef](#)] [[PubMed](#)]
46. Dundar, S.; Topkaya, T.; Solmaz, M.Y.; Yaman, F.; Atalay, Y.; Saybak, S.; Asutay, F.; Cakmak, O. Finite element analysis of the stress distributions in peri-implant bone in modified and standard-threaded dental implants. *Biotechnol. Biotechnol. Equip.* **2016**, *30*, 127–133. [[CrossRef](#)]
47. Greenstein, G.; Greenstein, B.; Carpentieri, J. The Need to Replace a Missing Second Molar With a Dental Implant Restoration: Analysis of a Controversial Issue. *Compend. Contin. Educ. Dent.* **2018**, *39*, 686–693. [[PubMed](#)]
48. Yoshitani, M.; Takayama, Y.; Yokoyama, A. Significance of mandibular molar replacement with a dental implant: A theoretical study with nonlinear finite element analysis. *Int. J. Implant. Dent.* **2018**, *4*, 4. [[CrossRef](#)] [[PubMed](#)]